Available online at www.sciencedirect.com
SCIENCE DIRECT®
Journal of Solid State Chemistry 173 (2003) 101–108
JOURNAL OF SOLID STATE CHEMISTRY
http://elsevier.com/locate/jssc

A new vanadium(III) fluorophosphate with ferromagnetic interactions, $(NH_4)[V(PO_4)F]$

Estibaliz Alda,[a] Begoña Bazán,[b] José L. Mesa,[a] José L. Pizarro,[b] María I. Arriortua,[b] and Teófilo Rojo[a,*]

[a] *Departamento de Química Inorgánica, Facultad de Ciencias, Universidad del País Vasco, Apdo. 644, E-48080 Bilbao, Spain*
[b] *Departamento de Mineralogía-Petrología, Facultad de Ciencias, Universidad del País Vasco, Apdo. 644, E-48080 Bilbao, Spain*

Received 23 October 2002; received in revised form 10 January 2003; accepted 31 January 2003

Abstract

A new vanadium(III) phosphate, $(NH_4)[V(PO_4)F]$, has been synthesized by using mild hydrothermal conditions under autogeneous pressure. The crystal structure has been solved from X-ray single crystal data. The compound crystallizes in the *Pnna* orthorhombic space group, with the unit-cell parameters $a = 12.982(2)$, $b = 10.608(1)$, $c = 6.4789(6)$ Å and $Z = 8$. The final R factors were $R_1 = 0.077$ [all data] and $wR_2 = 0.068$. The crystal structure consists of a three-dimensional framework formed by VO_4F_2 octahedra and tetrahedral $(PO_4)^{3-}$ phosphate anions. The vanadium(III) cations from the VO_4F_2 octahedra are linked through the fluorine atoms giving rise to zig-zag chains. The ammonium cations are located in the cavities of the structure compensating the anionic charge of the $[V(PO_4)F]^-$ inorganic skeleton. The IR spectrum shows the characteristic bands of the phosphate anion. The diffuse reflectance spectroscopy allowed us to calculate the Dq and Racah parameters. The values are $Dq = 1540$, $B = 505$ and $C = 2460\,cm^{-1}$. Magnetic measurements indicate the existence of weak ferromagnetic interactions.

Keywords: Hydrothermal synthesis; V(III) phosphates; Crystal structure; Ferromagnetism

1. Introduction

The research on phosphate materials with new open frameworks is currently in progress due to their potential applications in catalysis, gas separation, ion exchangers [1,2]. The study of phosphates of transition elements with low oxidation states has received great interest in recent years. The great ability of the phosphate frameworks to stabilize reduced oxidation states is a consequence of the relatively high charge in the $(PO_4)^{3-}$ tetrahedral that favours the formation of anionic frameworks with a high degree of mechanical, chemical and thermal stability. The vanadium phosphate systems are of interest for their different structural, catalytic and magnetic characteristics. V–O–P materials containing PO_4, HPO_4, H_2PO_4 or P_2O_7 tetrahedra [3], and the vanadium metal in different oxidation states are now known [4]. It is worth mentioning, the vanadyl phosphate phases which shown a rich intercalation chemistry, with the possible conversion to porous materials [5]. Furthermore, the vanadyl pyrophosphate is today used as catalyst for the oxidation of butane to maleic anhydride [6].

In the last years, both organically templated and inorganic–organic hybrid vanadium phases with open frameworks have been reported [1]. The organically templated compounds were synthesized from soft hydrothermal conditions using alkyldiamines as structural directing agents. In this way, mixed valence vanadium compounds with the ethylenediammonium [7] and pyperazinium [8] cations acting as counterions of the inorganic open-skeleton are known. Fluorophosphate compounds belonging to these kinds of compounds with vanadium(IV) and vanadium(V) cations have been recently reported [9,10]. Furthermore, inorganic–organic hybrid vanadium phosphates with a directly coordinated organonitrogen ligand such as the 2,2′-bipyridine or the 2,2′:6′,2″-terpyridne are also known [11].

Up to day, few vanadium(III) phosphates have been synthesized and studied. A rubidium vanadium(III)

*Corresponding author. Fax: +34-944648500.
E-mail address: qiproapt@lg.ehu.es (T. Rojo).

0022-4596/03/$ - see front matter © 2003 Elsevier Science (USA). All rights reserved.
doi:10.1016/S0022-4596(03)00098-7

borophosphate with chain structure has been reported [12]. The (4,4′-H_2bpy)[$V_2(HPO_4)_4$(4,4′-bpy)$_2$] and [$(C_2N_2H_9)V(PO_4)F$] phases exhibit a mixed inorganic–organic layered structure [13]. The crystal structure of the later compound shows $[V(PO_4)F]^-$ anionic sheets formed by VO_3F_2N octahedra which give rise to interconnected chains along the *b*-axis, with antiferromagnetic interactions [13c]. Finally, a three-dimensional (3D) vanadium(III) borophosphate that exhibits channels occupied by cesium cations is also known, but its magnetic behavior has not been described [14].

In this work, we report on the hydrothermal synthesis of a new 3D vanadium(III) phase, $(NH_4)[V(PO_4)F]$. The crystal structure, spectroscopic and magnetic properties of this compound are also reported. This compound is the first example in the $(NH_4)[M(PO_4)F]$ materials [15] that exhibits ferromagnetic interactions.

2. Experimental section

2.1. Synthesis and chemical analysis

$(NH_4)[V(PO_4)F]$ has been synthesized by using mild hydrothermal conditions under autogeneous pressure. The reagents V_2O_3, $H_3(PO_4)$ and HF, in a molar ratio of 1:4:42, and ammonium hydroxide up to pH of 6.0 were solved in water. This reaction mixture, with a total volume of 30 mL, was stirred up to homogeneity and sealed in a PTFE-lined stainless steel pressure vessel (fill factor 75%). After 5 days of reaction at 170°C green single-crystals appeared, being the yield of 85%. They were isolated by filtration, washed with water and acetone and dried over P_2O_5 for 2 h.

The percentage of the elements in the $(NH_4)[V(PO_4)F]$ product was calculated by inductively coupled plasma atomic emission spectroscopy (ICP-AES) and N-elemental analysis. Fluorine content was determined using a selective electrode. Found: V, 27.6; P, 16.6; N, 7.3; H, 2.0; F, 9.9. $(NH_4)[V(PO_4)F]$ requires V, 27.8; P, 16.9; N, 7.6; H, 2.2; F, 10.4. The density, measured by flotation in a mixture of $CHCl_3/CH_2I_2$, was of 2.6(2) g cm^{-3}.

2.2. Structural characterization

A prismatic single-crystal of $(NH_4)[V(PO_4)F]$ with dimensions 0.30 × 0.20 × 0.05 mm. was carefully selected under a polarizing microscope and mounted on a glass fiber. The diffraction data were collected at room temperature on an Enraf–Nonius CAD4 automated diffractometer using graphite-monochromated Mo*K*α radiation. Details of crystal data, intensity collection and some features of the structure refinement are reported in Table 1. Lattice constants were obtained by a least-squares refinement of the setting angles of 25 reflections in the range $5° < \theta < 15°$. Intensities and angular positions of two standard reflections were measured every hour and showed neither decrease nor misalignment during data collection.

Table 1
Crystallographic data and details of the crystal structure refinement for the $(NH_4)[V(PO_4)F]$ compound

Chemical formula	$(NH_4)[V(PO_4)F]$
Formula weight (g mol^{-1})	182.92
a (Å)	12.982(2)
b (Å)	10.608(1)
c (Å)	6.4789(6)
V (Å^3)	892.2(2)
Z	8
Space group	*Pnna* (no. 52)
T (°C)	293
Radiation, λ(Mo*K*α), Å	0.71073
$\rho_{obsd.}$, $\rho_{calcd.}$, g cm^{-3}	2.6(2), 2.664
μ(Mo*K*α) mm^{-1}	2.521
Data/parameters	902/75
$R[I > 2\sigma(I)]$	$R_1 = 0.030$, w$R_2 = 0.058$
R [all data]	$R_1 = 0.077$, w$R_2 = 0.068$
GOF	0.983

$R_1 = [\sum(|F_o| - |F_c|)]/\sum|F_o|$; $wR_2 = [\sum[w(|F_o|^2 - |F_c|^2)^2]/\sum[w(|F_o|^2)^2]]^{1/2}$; $w = 1/[\sigma^2|F_o|^2 + (xp)^2]$; where $p = [|F_o|^2 + 2|F_c|^2]/3$; $x = 0.0293$.

1761 reflections were measured in the range $3.84° \leqslant \theta \leqslant 26.36°$. A total of 902 were independent [$R_{int.} = 0.0519$] and 582 observed applying the criterion $I > 2\sigma(I)$. Corrections for Lorentz and polarization effects were done and also for absorption with the empirical ψ scan method [16] by using the X-RAYACS program [17]. The structure was solved by direct methods (SHELXS 97 program) [18] and refined by full-matrix least-squares based on F^2, using the SHELXL 97 computer program [19]. The scattering factors were taken from Ref. [20]. The unit-cell parameters of $(NH_4)[V(PO_4)F]$ are close to those found for the $KTiO(PO_4)$-type materials [15]. So, and taking into account that the space group utilized to describe the $KTiO(PO_4)$-type structures [15] is the acentric $Pna2_1$ (abc) we initially considered the solution of the crystal structure of $(NH_4)[V(PO_4)F]$ in this space group. The $[V(PO_4)F]^-$ inorganic skeleton could be unambiguously located in the Fourier maps and the ammonium cations were placed in two different crystallographic positions. However, the structural model obtained in this space group can not be correctly refined. The temperature factors of several non-hydrogen atoms were not defined, being the correlation factors between the atomic coordinates too high. These results can be attributed to the small number of observed reflections due to the low quality of the single-crystals, which leads to a slow reflection:variable ratio (902:145). The final *R* factors were $R_1 = 0.103$ (all data) and w$R_2 = 0.076$. These facts precluded us to present a reasonable good refinement of the crystal structure of $(NH_4)[V(PO_4)F]$ in the $Pna2_1$ space group. Alternatively, we consider the structural

resolution in the centric *Pnna* (acb) space group. The structure of the $[V(PO_4)F]^-$ inorganic skeleton was maintained invariable in relation with that obtained when the $Pna2_1$ space group is considered. However, the ammonium cations must be considered as disordered with occupancy factors of 50%, and a pseudo-inversion center appears at $x = \frac{1}{4}$, $y = \frac{1}{4}$, $z = 0.290$ relating the $[V(PO_4)F]^-$ units. All non-hydrogen atoms were assigned anisotropic thermal parameters. Hydrogen atoms of the ammonium cations could not be located in the Fourier maps. The reflection:variable ratio is 902:75. The final R factors are $R_1 = 0.077$ and $wR_2 = 0.068$. In the final difference synthesis maximum and minimum peaks of 0.473, $-0.424\,e\,Å^{-3}$ were found. So, although the characteristic space group of the $KTiO(PO_4)$-type materials is the $Pna2_1$, particularly the crystal structure of $(NH_4)[V(PO_4)F]$ could only be reasonably refined in the centric *Pnna* space group. The CSD depository number is 391,166. A simulation based on the $(NH_4)[V(PO_4)F]$ single-crystal structure was in excellent agreement with the X-ray powder data, indicating phase purity and high crystallinity. The drawings of the crystal structure were performed using ATOMS program [21]. Atomic coordinates and selected bond distances and angles are listed in Tables 2 and 3.

2.3. Physical measurements

Thermogravimetric analysis was carried out under air atmosphere in a SDC 2960 Simultaneous DSC-TGA TA Instrument. A crucible containing ca. 20 mg of sample was heated at $5°C\,min^{-1}$ in the temperature range 30–800°C. The X-ray thermodiffractometry was performed in a PHILIPS X'PERT automatic diffractometer (Cu$K\alpha$ radiation) equipped with a variable-temperature stage (Paar Physica TCU2000) with a Pt sample holder. The powder patterns were recorded in 2θ steps of 0.02° in the range $5 \leqslant 2\theta \leqslant 40°$, counting for 2 s per step and increasing the temperature at $5°C\,min^{-1}$ from room temperature up to 800°C. The IR spectrum (KBr pellet) was obtained with a Mattson Satellite FTIR spectrophotometer in the 400–4000 cm^{-1} range. Diffuse reflectance spectrum was registered at room temperature on a Cary 2415 spectrometer in the 210–2000 nm range. Magnetic measurements on powdered sample were performed in the temperature range 2.0–300 K, using a Quantum Design MPMS-7 SQUID magnetometer. The magnetic field was 0.1 T, a value in the range of linear dependence of magnetization vs. magnetic field even at 2.0 K.

Table 2
Atomic coordinates ($\times 10^4$) and equivalent temperature factors ($Å^2 \times 10^3$) for $(NH_4)[V(PO_4)F]$ (e.s.d. in parentheses)

Atom	x	y	z	U_{eq}
V(1)	1341(1)	2500	7500	7(1)
V(2)	0	0	0	8(1)
P(1)	675(1)	2500	2500	8(1)
P(2)	2500	0	−793(2)	9(1)
F(1)	−238(2)	−1239(2)	2208(4)	18(1)
O(1)	−31(2)	1368(3)	2050(4)	12(1)
O(2)	1540(2)	−212(3)	522(4)	11(1)
O(3)	1352(2)	2211(2)	4381(4)	14(1)
O(4)	2345(2)	1150(2)	−2206(4)	15(1)
N(1)	1510(6)	6796(8)	1067(1)	38(2)
N(2)	1427(8)	574(1)	1031(2)	38(2)

$U_{eq} = (1/3)\sum_i \sum_j U_{ij} a_i^* a_j^* \mathbf{a_i}.\mathbf{a_j}$.

Table 3
Selected bond distances (Å) and angles (°) for $(NH_4)[V(PO_4)F]$ (e.s.d. in parentheses)

Bond distances (Å)			
$V(1)O_4F_2$ *octahedron*		$V(2)O_4F_2$ *octahedron*	
V(1)–F(1)^{i,ii}	1.968(2) × 2	V(2)–F(1)^{o,vi}	1.967(3) × 2
V(1)–O(3)^{o,iii}	2.044(3) × 2	V(2)–O(1)^{o,vi}	1.968(3) × 2
V(1)–O(4)^{iv,v}	1.946(3) × 2	V(2)–O(2)^{o,vi}	2.040(2) × 2
$P(1)O_4$ *tetrahedron*		$P(2)O_4$ *tetrahedron*	
P(1)–O(1)^{o,iv}	1.538(3) × 2	P(2)–O(2)^{o,vii}	1.526(2) × 2
P(1)–O(3)^{o,iv}	1.534(3) × 2	P(2)–O(4)^{o,vii}	1.539(3) × 2
Ammonium cation			
N(1)···N(2)	1.15(1)		
Hydrogen contact distances			
N(1)···O(3)	2.810(8)	N(1)···O(4)	2.776(9)
N(1)···F(1)	2.719(8)	N(1)···O(2)	2.987(9)
N(2)···O(4)	2.60(1)	N(2)···F(1)	2.75(1)
N(2)···O(2)	2.76(1)	N(2)···O(1)	2.86(1)
Interpolyhedral bond angles (°)			
V(2)–F(1)–V(1)^{i}	129.6(1)	P(1)–O(1)–V(2)	133.7(2)
P(2)–O(2)–V(2)	133.7(1)	P(1)–O(3)–V(1)	138.7(2)
P(2)–O(4)–V(2)^{viii}	136.8(2)		

Symmetry codes: o $= x, y, z$; i $= -x, -y, -z+1$; ii $= -x, y+1/2, z+1/2$; iii $= x, -y+1/2, -z+3/2$; iv $= x, -y+1/2, -z+1/2$; v $= x, y, z+1$; vi $= -x, -y, -z$; vii $= -x+1/2, -y, z$; viii $= x, y, z-1$.

3. Results and discussion

3.1. Description of the structure

The crystal structure of $(NH_4)[V(PO_4)F]$ consists of a 3D network constructed from corner-sharing of VO_4F_2 octahedra and PO_4 tetrahedra (Fig. 1a). The structure shows the existence of interconnected zig-zag chains formed by VO_4F_2 octahedra linked through fluorine atoms along the |011| and |0−11| directions (Fig. 1b). This architecture delimits six-ring channels running along the *a*- and *c*-axis in which the disordered ammonium cations are located (Fig. 1a). These groups compensate the anionic charge of the $[V(PO_4)F]^-$

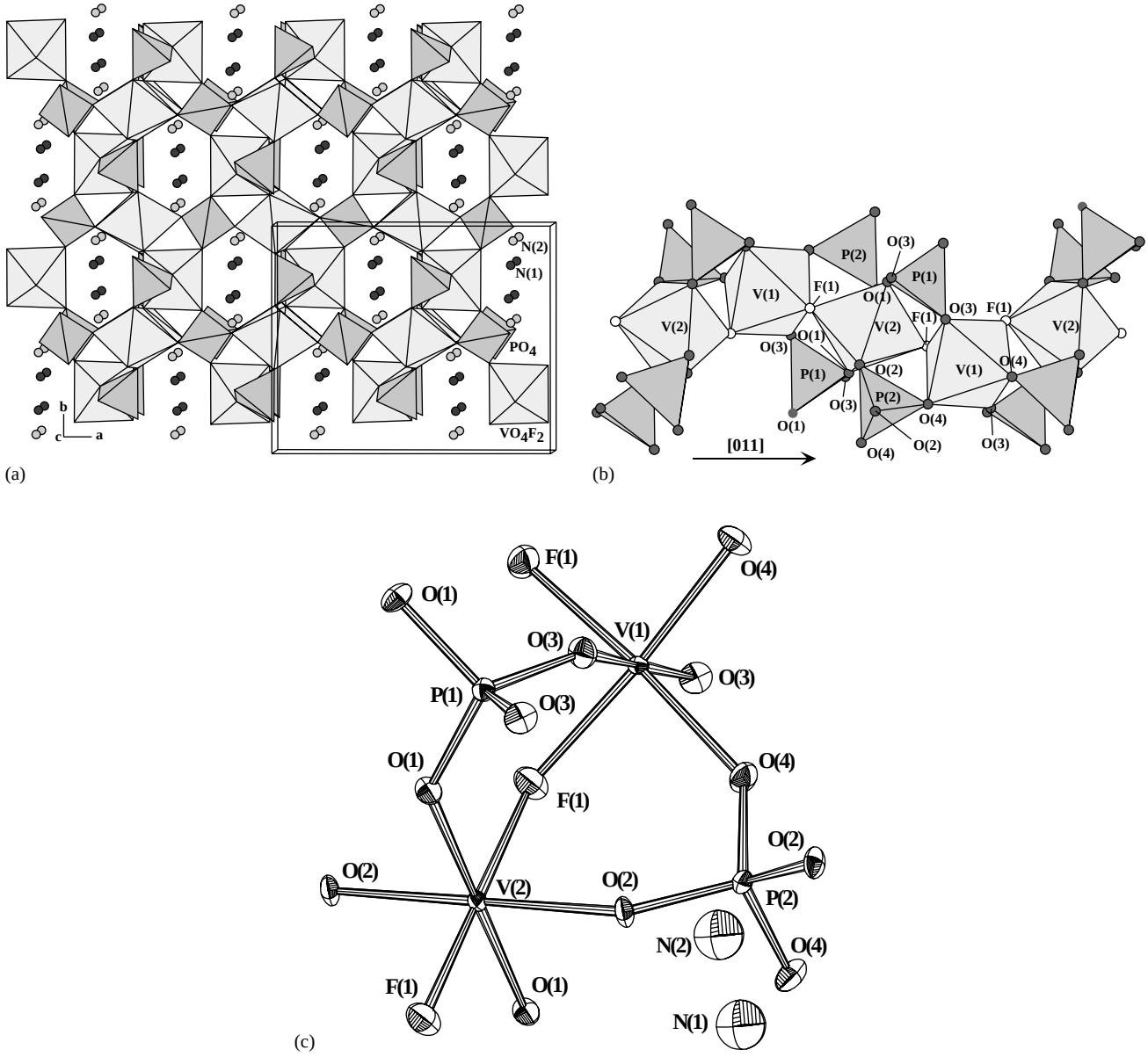

Fig. 1. Polyhedral view of the crystal structure of $(NH_4)[V(PO_4)F]$ showing (a) the 3D framework and (b) the zig-zag chains. (c) ORTEP drawing showing the asymmetric unit and the atom labelling.

inorganic skeleton and establish hydrogen bonds with the fluorine and oxygen atoms of the VO_4F_2 octahedra.

The asymmetric unit of $(NH_4)[V(PO_4)F]$ consists of two PO_4 tetrahedra that share two corner-oxygen atoms with two different VO_4F_2 octahedra (Fig. 1c). The $V(1)O_4F_2$ and $V(2)O_4F_2$ octahedra are linked together via the F(1)-fluorine atom. In both octahedra the vanadium(III) cations are linked to the oxygen atoms belonging to the PO_4 tetrahedra with a mean V–O bond distance of 2.00(5) Å. The hexacoordination is completed with two fluorine ions bonded at a mean distance of 1.967(3) Å. The *cis*- and *trans*-O–V–O bond angles are near to 90° and 180°, respectively, as expected for a slightly distorted octahedral geometry around the vanadium(III) cations (Fig. 1c).

The phosphorous atoms are in tetrahedral coordination with average P–O distance of 1.534(6) Å and O–P–O angles near 110°, as expected in the phosphate compounds. The hydrogen bonds established between the ammonium cations and the fluorine and oxygen atoms of the $[V(PO_4)F]^-$ network are in the 2.60(1)–2.99(1) Å range.

The existence of iron(III) and gallium(III) phosphates belonging to the $(NH_4)[M(PO_4)F]$ family with KTiO(PO_4) structure-type is described in Ref. [15]. Although the crystal structure of $(NH_4)[V(PO_4)F]$ was solved in a different space group than the other phases (Table 4), all these compounds can be considered isotypic with the same $[M(PO_4)F]^-$ inorganic framework. Thus, the volume of the unit-cell in this series of compounds

Table 4
Unit-cell parameters and M–F–M intermetallic angle for the $(NH_4)[M(PO_4)F]$ (M = Ga, V and Fe) compounds

Compound	(NH_4) [Ga(PO$_4$)F]	(NH_4) [V(PO$_4$)F]	(NH_4) [Fe(PO$_4$)F]
Space group	$Pna2_1$	$Pnna$	$Pna2_1$
a (Å)	12.9207(2)	12.978(2)	12.993(3)
b (Å)	6.4400(1)	10.600(2)	6.468(1)
c (Å)	10.4147(2)	6.4797(7)	10.640(3)
V (Å)^3	866.60(3)	891.4(2)	894.2(6)
Z	8	8	8
Ionic radius M^{3+} (Å)	0.620	0.640	0.645
M–F–M angle (°)	130.0(1)	129.6(1)	129.4(1)

The ionic radii were taken from Ref. [22].

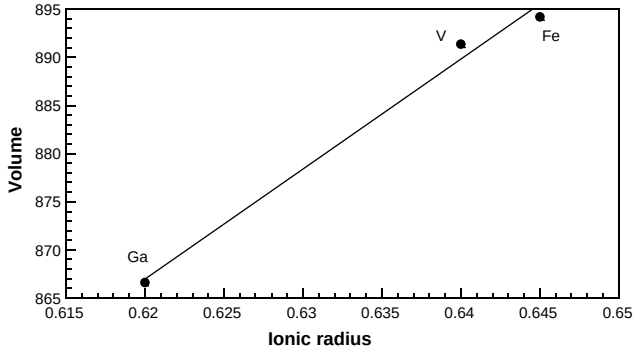

Fig. 2. Variation of the unit-cell volume vs. ionic radius for the $(NH_4)[M(PO_4)F]$ (M = Ga, V and Fe) compounds.

shows a linear increase with increasing the ionic radii from the gallium(III) to iron(III) phosphate [22], according to the Vegard's law (Fig. 2).

3.2. Thermal behavior

The thermal decomposition curve of $(NH_4)[V(PO_4)F]$ under air atmosphere shows a continuous weight loss of ca. 12% from ca. 200°C to 460°C. This loss can be attributed to the elimination of the ammonium cation (required loss, 9.8%) and the beginning of the loss of the fluorine anion. Above 460°C superimposed steps, with increasing and decreasing of mass, are observed in the thermogravimetric curve. These steps can be associated with chemical transformations of the inorganic residue. At 800°C an amorphous product that can not be identified by X-ray diffraction was obtained.

To know the phases present in the thermal decomposition of $(NH_4)[VF(PO_4)]$, time-resolved X-ray thermodiffractometry in air atmosphere was carried out. $(NH_4)[V(PO_4)F]$ is stable up to ca. 315°C, and the intensity of the monitored (210) and (011) superimposed peaks at $2\theta = 16.1^\circ$ remains practically unchanged (Fig. 3). In the 315–405°C range no peaks were observed in the diffractograms, which indicates that after the loss of the ammonium cation the crystal structure collapses and yields amorphous products. Above 405°C the $V(PO_3)_3$ phase is detected [Ic space group with $a = 10.61(1)$, $b = 19.09(1)$, $c = 9.43(1)$ Å and $\beta = 97.9(1)^\circ$] [23], giving rise to the β-$VO(PO_4)$ compound at ca. 555°C [$Pnma$ space group with $a = 7.78(1)$, $b = 6.13(1)$, $c = 6.97(1)$ Å] [22]. At temperatures of ca. 735°C the presence of $V_2(VO)(P_2O_7)_2$ [$Pnma$ space group with $a = 17.46(1)$, $b = 12.18(1)$, $c = 5.24(1)$ Å] is observed in the diffractograms [23]. Finally, at temperature near 800°C an amorphous melted product was obtained.

3.3. Infrared and UV–Vis spectroscopy

The infrared spectrum of $(NH_4)[V(PO_4)F]$ exhibits the bands corresponding to the vibrations of the ammonium cation and the $(PO_4)^{3-}$ phosphate oxoanion (Fig. 4). The stretching mode of the $(NH_4)^+$ group appears at 3235 cm^{-1}. The band near 1415 cm^{-1} can be assigned to the bending vibration of this cation. Three different groups of bands can be attributed to the vibrational

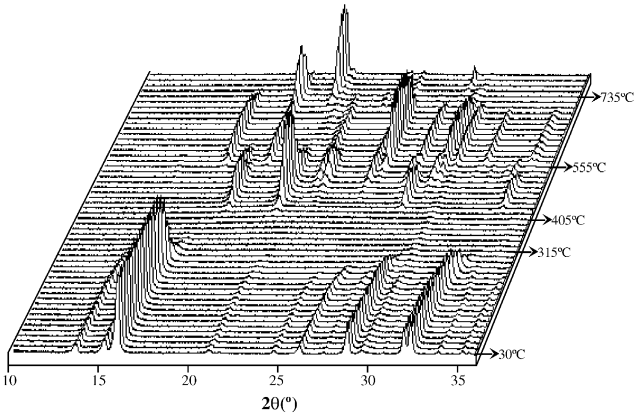

Fig. 3. Thermodiffractograms of $(NH_4)[V(PO_4)F]$.

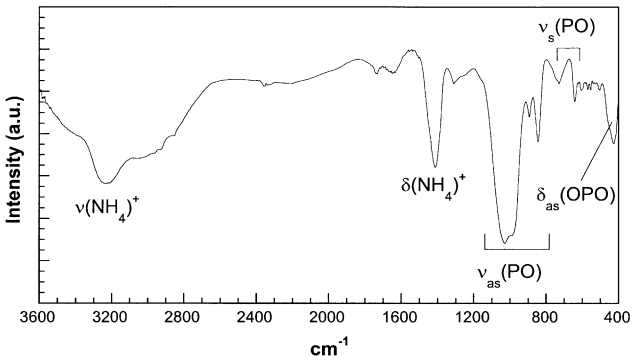

Fig. 4. IR spectrum of $(NH_4)[V(PO_4)F]$.

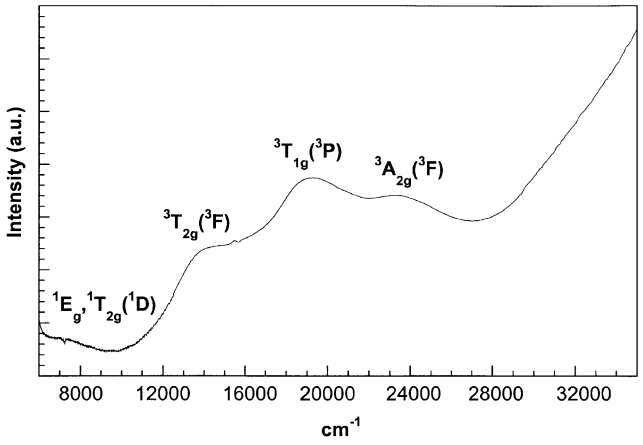

Fig. 5. Diffuse reflectance spectrum of $(NH_4)[V(PO_4)F]$.

modes of the $(PO_4)^{3-}$ anion [24]. The asymmetric ν_{as}(P–O) stretching mode appears at 1030, 980, 890 and 845 cm^{-1}. The symmetric ν_s(P–O) stretch is detected at 730 and 640 cm^{-1}. The asymmetric deformation vibration [δ_{as}(O–P–O)] is observed at 460 and 430 cm^{-1}. These results are similar to those found for other related phosphates [25].

The diffuse reflectance spectrum of $(NH_4)[V(PO_4)F]$ shows the spin allowed transitions from the fundamental state $^3T_{1g}(^3F)$ to the excited levels $^3T_{2g}(^3F)$, $^3T_{1g}(^3P)$ and $^3A_{2g}(^3F)$ at the frequencies 14,000, 20,000 and 24,000 cm^{-1}. Furthermore, the spin forbidden transition $^3T_{1g}(^3F) \rightarrow {}^1E_g(^1D), {}^1T_{2g}(^1D)$ was observed as a weak band at 8000 cm^{-1} (Fig. 5). The Dq and Racah parameters (B and C) were calculated by fitting the experimental frequencies to the energy expressions for a d^2 ion [26a]. The values obtained were $Dq = 1540\,cm^{-1}$, $B = 505\,cm^{-1}$ and $C = 2460\,cm^{-1}$. These results are in good agreement with those observed for the V(III) ion in slightly distorted octahedral environment [26]. The value obtained for the B-parameter is approximately 60% of that corresponding to the V^{3+} free ion (861 cm^{-1}), which indicates the existence of a significant covalence character in the V–O chemical bonds.

3.4. Magnetic properties

Magnetic measurements of $(NH_4)[V(PO_4)F]$ were performed on powdered sample from room temperature to 2.0 K. The thermal evolution of the χ_m^{-1} and $\chi_m T$ curves is shown in Fig. 6. The molar magnetic susceptibility, χ_m, increases with decreasing temperature in all the temperature range studied. Above ca. 50 K the thermal variation of the molar susceptibility follows a Curie–Weiss law [$\chi_m = C_m/(T-\theta)$] with values of the Curie and Curie–Weiss constants of 0.865 cm^3 K/mol and 2.7 K, respectively. The $\chi_m T$ vs. T curve continuously increases from 0.895 cm^3 K/mol at room temperature up to 3.417 cm^3 K/mol at 2.0 K. This result and the

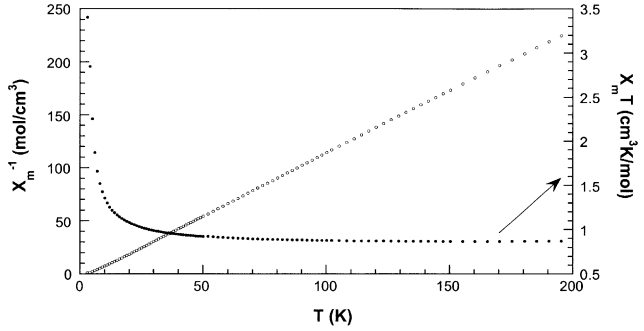

Fig. 6. Thermal variation of the χ_m^{-1} and $\chi_m T$ curves for $(NH_4)[V(PO_4)F]$.

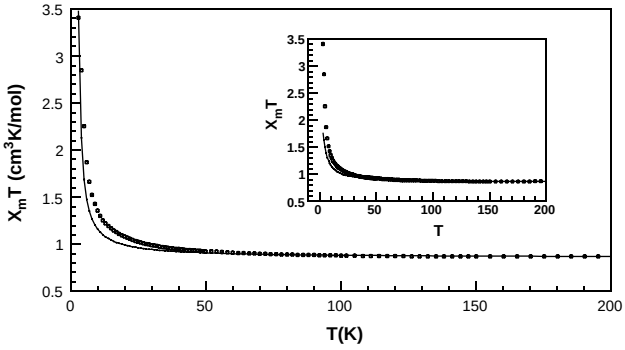

Fig. 7. Fit of the $\chi_m T$ curve of $(NH_4)[V(PO_4)F]$ to a 3D ferromagnetic model. The inset shows the fit to a model for chains. The solid lines represent the fit to the theoretical models.

small positive Weiss temperature indicate the existence of weak ferromagnetic exchange interactions in this compound. Magnetization measurements performed at 2 K do not show any hysteresis loop, being the magnetization of approximately 0.94 BM at 5 T, which is near to the value expected for a system with spin $S = 1$.

Taking into account the 3D network of $(NH_4)[V(PO_4)F]$, as described in the structural description, we have fitted the magnetic data to the expression derived by Rushbrooke and Wood for a ferromagnetic 3D simple cubic network of spin $S = 1$ [Eq. (1)] [27],

$$\chi_m = (2N\beta^2 g^2/3kT)(1 - 8.0x + 14.67x^2 - 14.22x^3 + 61.19x^4 - 162.45x^5 - 1127.96x^6)^{-1}, \quad (1)$$

where $x = |J|/kT$, k is the Boltzmann constant, N is Avogadro's number and β is the Bohr magneton. The results show a reasonable good fit with a J-exchange parameter of $|J/K| = 0.35$ K with $g = 1.85$ (see Fig. 7). On the other hand, and considering both that the effective magnetic moment at room temperature of $(NH_4)[V(PO_4)F]$ is close to the expected spin-only value and the structural features, attempts to fit the magnetic data to an isotropic chain model for spin $S = 1$ were

also carried out. The results are shown in the inset of Fig. 7. As can be seen in this figure, the fit is worst than that corresponding to the 3D model. This fact is probably due to the existence in the structure of interconnected chains that give rise to a magnetic behavior that corresponds with a near 3D ferromagnet.

A comparison between the $(NH_4)[V(PO_4)F]$ and $(NH_4)[Fe(PO_4)F]$ [15a] isotypic compounds shows the same kind of 3D framework with corner-sharing octahedra, in which the metallic cations are linked through fluorine ions with M–F–M angles of approximately 130° in both phases (see Table 4). However, the magnetic behavior of these compounds is quite different. In this way, the iron phosphate shows strong antiferromagnetic exchange interactions with a Weiss constant of approximately −230 K and an ordering temperature near to 75 K, whereas the vanadium phosphate is ferromagnetically coupled ($\theta = 2.7$ K, $|J/K| = 0.35$ K). The difference in sign of the magnetic interactions observed in these compounds could be associated with the reduction in the number of possible magnetic exchange pathways that takes place in the vanadium(III) d^2-cation in comparison with the d^5-high spin iron(III) compound [28]. Unlike this compound, the layered $[(C_2N_2H_9)V(PO_4)F]$ vanadium(III) phase exhibits an antiferromagnetic behavior which can not be fitted to any 1D, 2D, 3D magnetic models of spin $S = 1$ [13c]. These facts preclude the establishment of suitable magneto-structural correlations with the title compound.

4. Concluding remarks

The hydrothermal synthesis under autogeneous pressure allowed us to obtain the new $(NH_4)[V(PO_4)F]$ compound. The structure consists of a 3D network formed by VO_4F_2 octahedra and PO_4 tetrahedra giving rise to zig-zag chains. The crystal structure collapses after the loss of the ammonium cations at ca. 315°C. IR spectroscopy confirms the presence of the phosphate anion. The diffuse reflectance measurements show the presence of the vanadium(III) cations in slightly distorted octahedral geometry. Magnetic measurements indicate the existence of weak ferromagnetic couplings in the $(NH_4)[V(PO_4)F]$ compound. This phase is the first member found in the $(NH_4)[M(PO_4)F]$ family with $KTiO(PO_4)$ structure-type exhibiting ferromagnetic exchange interactions.

Acknowledgments

This work was financially supported by the Ministerio de Educación y Ciencia (BQU2001-0678) and Universidad del País Vasco/EHU (9/UPV00169.310-13494/2001; 9/UPV00130.310-13700/2001) which we gratefully acknowledge. One of us B. Bazan wishes to thank the Universidad del País Vasco/EHU for funding.

References

[1] A.K. Cheetham, G. Ferey, T. Loiseau, Angew. Chem. Int. Ed. 38 (1999) 3268.
[2] M.E. Davis, Chem. Eur. 3 (11) (1997) 1745.
[3] (a) K.H. Lii, H.J. Tsai, J. Solid State Chem. 91 (1991) 331.
(b) K.H. Lii, N.S. Wen, C.C. Su, B.R. Chen, Inorg. Chem. 31 (1992) 439.
(c) R.C. Haushalter, Z. Wang, M.E. Thompson, J. Zubieta, Inorg. Chim. Acta 232 (1995) 83.
(d) R.C. Haushalter, Z. Wang, M.E. Thompson, J. Zubieta, Inorg. Chem. 32 (1993) 3700.
(e) R.C. Haushalter, Z. Wang, M.E. Thompson, J. Zubieta, Inorg. Chem. 32 (1993) 3966.
(f) H.-J. Koo, M.-H. Whangbo, P.D. VerNooy, C.C. Torardi, W.J. Marshall, Inorg. Chem. 41 (2002) 4664.
(g) A. Leclaire, M.M. Borel, B. Raveau, J. Solid State Chem. 162 (2001) 354.
[4] (a) K.H. Lii, H.J. Tsai, J. Solid State Chem. 90 (1991) 291.
(b) K.H. Lii, L.F. Mao, J. Solid State Chem. 96 (1992) 436.
(c) R. Haushalter, V. Soghomanian, Q. Chen, J. Zubieta, J. Solid State Chem. 105 (1993) 512.
(e) N. Henry, O. Mentre, F. Abraham, J. Solid State Chem. 163 (2002) 519.
[5] (a) L. Benes, V. Zima, K. Melanova, M. Trchova, P. Capkova, B. Koudelka, P. Matejka, Chem. Mater. 14 (2002) 2788.
(b) B.G. Shpeizer, X. Ouyang, J. Heising, A. Clerfield, Chem. Mater. 13 (2001) 2288.
[6] J. Do, P.R. Bontchev, A.J. Jacobson, Chem. Mater. 13 (2001) 2601.
[7] V. Soghomanian, Q. Chen, R.C. Haushalter, J. Zubieta, Angew. Chem. Int. Ed. 32 (1993) 610.
[8] J. Do, R.P. Bontchev, A.J. Jacobson, J. Solid State Chem. 154 (2000) 514.
[9] D. Riou, G. Ferey, J. Solid State Chem. 111 (1994) 422.
[10] G. Bonavia, R.C. Haushalter, J. Zubieta, J. Solid State Chem. 126 (1996) 292.
[11] (a) Y. Lu, E. Wang, M. Yuan, G. Luan, Y. Li, H. Zhang, C. Hu, Y. Yao, Y. Qin, Y. Chen, J. Chem. Soc., Dalton Trans. (2002) 3029.
(b) R.C. Finn, J. Zubieta, J. Chem. Soc., Dalton Trans. (2002) 856.
[12] H. Engelhardt, H. Borrmann, R. Kniep, Z. Kristallogr. 215 (2000) 203.
[13] (a) C.-H. Huang, L.-H. Huang, K.-H. Lii, Inorg. Chem. 40 (2001) 2625.
(b) M. Riou-Cavellec, C. Serre, G. Ferey, C. R. Acad. Sci. Paris t. 2 (S. II) (1999) 147.
(c) E. Alda, S. Fernandez, J.L. Mesa, J.L. Pizarro, V. Jubera, T. Rojo, Mater. Res. Bull. 37 (2002) 2355.
[14] H. Engelhardt, H. Borrmann, W. Schnelle, R. Kniep, Z. Anorg. Allg. Chem. 626 (2000) 1647.
[15] (a) Th. Loiseau, Y. Calage, P. Lacorre, G. Ferey, J. Solid State Chem. 111 (1994) 390.
(b) I. Tordjman, R. Masse, J.C. Guitel, Z. Kristallogr. 139 (1974) 103.
(c) T. Loiseau, C. Paulet, N. Simon, V. Munch, F. Taulle, G. Ferey, Chem. Mater. 12 (2000) 1393.
[16] A.C.T. North, D.C. Philips, F.S. Mathews, Acta Crystallogr. A 24 (1968) 351.

[17] A. Chandrasekaran, X-RAYACS: Program for Single Crystal X-ray Data Corrections, Chemistry Department, University of Massachusetts, Amherst, USA, 1998.
[18] G.M. Sheldrick, SHELXS 97: Program for the Solution of Crystal Structures, University of Göttingen, Germany, 1997.
[19] G.M. Sheldrick, SHELXL 97: Program for the Refinement of Crystal Structures, University of Göttingen, Germany, 1997.
[20] International Tables for X-ray Crystallography", Kynoch Press, Birmingham, England, Vol. IV, 1974, p. 99.
[21] E. Dowty, ATOMS: A Computer Program for Displaying Atomic Structures, Shape Software, 521 Hidden Valley Road, Kingsport, TN, 1993.
[22] R.D. Shannon, Acta Crystallogr. A 32 (1976) 751.
[23] Powder Diffraction File-Inorganic and Organic, ICDD Files 83-1953, 27-948 and 79-41, Pennsylvania, 1995.
[24] K. Nakamoto, Infrared and Raman Spectra of Inorganic and Coordination Compounds, John-Wiley & Sons, New York, 1977.
[25] J. Escobal, J.L. Pizarro, J.L. Mesa, L. Lezama, R. Olazcuaga, M.I. Arriortua, T. Rojo, Chem. Mater. 12 (2000) 376.
[26] (a) A.B.P. Lever, Inorganic Electronic Spectroscopy, Elsevier Science, Amsterdam, Netherlands, 1984.
(b) W.R. Mason, H.B. Gray, J. Am. Chem. Soc. 90 (1968) 5721.
(c) J.E. Sutton, H. Krentzien, H. Taube, Inorg. Chem. 19 (1980) 2425.
[27] G.S. Rushbrooke, P.J. Wood, Mol. Phys. 1 (1958) 257.
[28] J.B. Goodenough, Magnetism and the Chemical Bond, Interscience, New York, 1963.